Physics Letters A 377 (2013) 2052–2057

Contents lists available at SciVerse ScienceDirect

Physics Letters A

www.elsevier.com/locate/pla

Competition between unlimited and limited energy growth in a two-dimensional time-dependent billiard

Diego F.M. Oliveira *, Thorsten Pöschel

Institute for Multiscale Simulations, Friedrich-Alexander Universität, D-91052 Erlangen, Germany

ARTICLE INFO

Article history:
Received 22 February 2013
Received in revised form 13 June 2013
Accepted 17 June 2013
Available online 21 June 2013
Communicated by A.R. Bishop

Keywords:
Chaos
Lorentz gas
Billiards
Scaling
Dissipation

ABSTRACT

Some dynamical properties for a dissipative time-dependent Lorentz gas are studied. We assume that the size of the scatterers change periodically in time. We show that for some combination of the control parameters the particles come to a complete stop between the scatterers, but for some other cases, the average velocity grows unbounded. This is the first time that the unlimited energy growth is observed in a dissipative system. Finally, we study the behavior of the average velocity as a function of the number of collisions and we show that the system is scaling invariant with scaling exponents well defined.

1. Introduction

The process in which a particle acquires unlimited energy is called Fermi acceleration. As an attempt to explain the origin of cosmic ray acceleration, Enrico Fermi [1] proposed that charged particles could be accelerated by interactions with time-dependent magnetic structures in the interstellar medium. Since his pioneering work many alternative models have been proposed in different fields such as molecular physics [2], optics [3], nanostructures [4], quantum dots [5] and many other. Additionally, different procedures have been used to describe such a systems and two main different approaches are considered, namely (i) by solving ordinary/partial differential equations or; (ii) by using the so-called billiard formalism. A billiard is a dynamical system in which one or many non-interacting particles move freely inside a closed region experiencing collisions with the boundary. From the mathematical point of view, a billiard is defined by a connected region $Q \subset R^D$, with boundary $\partial Q \subset R^{D-1}$ which separates Q from its complement, in such a case, the absolute velocity of the particle is constant. Basically billiards are classified as (i) integrable, (ii) ergodic and (iii) mixed. In case (i) the phase space consists of invariant spanning curves filling the entire phase space and typical examples are the circular [6] and the elliptical [7] billiards whose integrability in the case of the circle comes from the angular momentum conservation, and the product of the angular momenta with respect to the foci in case of ellipse. In case (ii) the time evolution of a single initial condition is enough to fill the phase space and three examples are the Bunimovich stadium [8], the Sinai billiard [9] and the cardioid billiard [10]. In case (iii), one important property in the mixed phase space is that chaotic seas are generally surrounding Kolmogorov–Arnold–Moser (KAM) islands which are confined by invariant curves [11–21]. In particular such curves can cross the phase plane and partition it into several separated portions of the phase space. On the other hand, if $\partial Q = \partial Q(t)$, the system has a time-dependent boundary, it can exchange energy with the particle upon collision and the velocity can increase or decrease depending on the phase of the moving boundary. One of the main questions about two-dimensional time-dependent systems is: Under which circumstances an unlimited energy growth will be observed? In this sense, Loskutov, Ryabov, and Akinshin [22] proposed a conjecture which was later proved by Gelfreich and Turaev [23,24]. This conjecture, known as LRA-conjecture, states that if there exists a chaotic component in the phase space with static boundary the introduction of a time-dependent perturbation is a sufficient condition to observe Fermi acceleration. Such a conjectures has been verified for the Bunimovich stadium [8,25], oval billiard [26], Sinai billiard [8]. However, it has been shown very recently that the existence of a chaotic component is a sufficient but not necessary condition the observe the unlimited energy growth, since Fermi acceleration was also observed for the time-dependent elliptic billiards (which is integrable for the static boundary) [27–32].

When dissipation is introduced into the system, a drastic change is observed in the phase space [33–40]. Invariant spanning

* Corresponding author. Tel.: +49 9131 85 20867.
E-mail addresses: diegofregolente@gmail.com (D.F.M. Oliveira), thorsten.poeschel@eam.uni-erlangen.de (T. Pöschel).

0375-9601/$ – see front matter
http://dx.doi.org/10.1016/j.physleta.2013.06.029

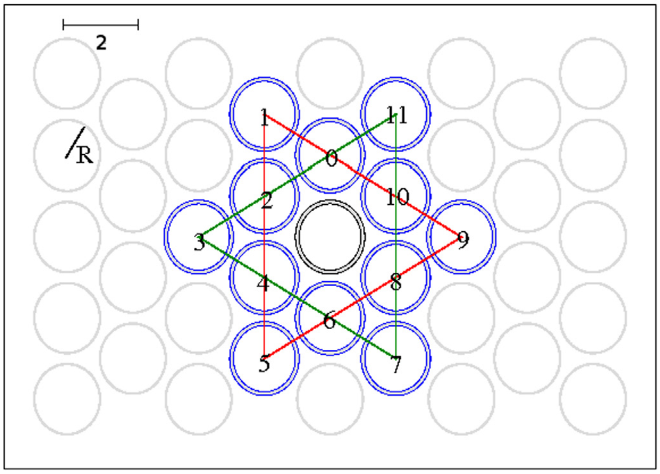

Fig. 1. Illustration of the time-dependent Lorentz gas.

curves are destroyed; the elliptic fixed points may turn into sinks and the chaotic sea can be eventually replaced by a chaotic attractor. Each one of these attractors has its own basin of attraction. Much attention has been devoted to dissipative systems and extensive research has been done to explain phenomena present in different fields of science including optics [41], fluid dynamics [42] and nanotechnology [43] among others. However, the influence of dissipation on the average velocity/energy of time-dependent systems is still not fully understood and one of the main questions that rises is: Is it possible to observe the unlimited energy in a dissipative system? As we will show, the answer is not so simple and it depends on the kind of the dissipative force, and the combination of the initial conditions and the control parameters.

We revisit the problem of a time-dependent Lorentz gas seeking to describe and understand the behavior of the average velocity for an ensemble of non-interacting particles as a function of both the control parameters and the number of collisions of the particles with the boundary. We assume a triangular arrangement in order to avoid particles traveling infinitely far from the scatterers. We show that the system has a ergodic phase space and we introduce time-dependent perturbation of breathing type on the boundary. In such a case the size of the scatterers change harmonically in time. Additionally, we introduce in-flight dissipation into the system where the dissipative force is given by $F = -\mu$ where μ is the dissipation parameter. We study the behavior of the average velocity for the parameter space and we shown that for some combination of the initial condition and the control parameter the particles come to a complete stop between the scatterers. On the other hand, for other combinations of control parameters and initial conditions the average velocity grows unbounded. It is important to emphasize that this is the first time that the unlimited energy growth is observed in a dissipative system. For such a case we show that the system is scaling invariant with exponents well defined.

The Letter is organized as follows. In Section 2 we describe all the necessary details to obtain the four-dimensional map that describes the dynamics of the system. Section 3 is devoted to the numerical results. Finally, conclusions are drawn in Section 4.

2. The model and the map

In this section we describe the model and all the details needed to obtain the map that describes the dynamics of the system. The model consists of classical non-interacting particles of mass m experiencing collisions with time-dependent circular scatters as can be seem in Fig. 1. The system is described in terms of a four-dimensional mapping $T(\delta_n, b_n, |\vec{V}_n|, t_n) = (\delta_{n+1}, b_{n+1}, |\vec{V}_{n+1}|, t_{n+1})$ where the dynamical variable δ_n angular position of the particle on the scatter; b_n is the impact parameter; $|\vec{V}_n|$ is the absolute velocity of the particle after collision and t_n is the time. Additionally, we assume that the dissipative force is given by $F = -\mu$ where μ is the dissipation parameter. In order to know the velocity of the particle as a function of time we need to solve Newton's equation. Thus the velocity of the particle as a function of time is given by

$$\left|\vec{V}_p(t)\right| = V_n - \mu(t - t_n), \tag{1}$$

where $V_n = |\vec{V}_n|$. Integrating Eq. (1) we obtain the trajectory as

$$r(t) = r_n + V_n(t - t_n) - \frac{1}{2}\mu(t - t_n)^2. \tag{2}$$

The dynamics starts on the scatterer in the center and the particle travels in a straight line until the next collision with one of the other 12 scatterers enumerated from zero to eleven. Moreover, we introduce the variable $l(s_n)$ for the distance between the center of the scatterer in the center and the scatterer hit at the collision $n+1$. $l(s_n)$ can assume the values of $4/\sqrt{3}$ and 4 for even and odd values of s_n, respectively. Additionally, we assume that the size of the scatterers change periodically in time according to

$$R = 1 + \epsilon\left[1 + \cos(t)\right], \tag{3}$$

where ϵ is the amplitude of the time-dependent perturbation. Starting with an initial condition $(\delta_0, b_0, V_0, t_0)$, the map that describes the dynamics of the system is obtained as follows. The Cartesian components of R are given by

$$X(\delta_n, t_n) = \left\{1 + \epsilon\left[1 + \cos(t)\right]\right\}\cos(\delta_n), \tag{4}$$

$$Y(\delta_n, t_n) = \left\{1 + \epsilon\left[1 + \cos(t)\right]\right\}\sin(\delta_n), \tag{5}$$

where δ_n is the angular position which is given by $\delta_n = \pi/2 + \theta_n - \arcsin(b_n/R)$ (see Fig. 2). Since we already know the angle that the particle's trajectory does with the horizontal $(\theta_n + \pi/2)$ and the position of the hit at the collision nth, we can obtain the vector velocity of the particle that is written as

$$\vec{V}_n = |\vec{V}_p|\left[-\sin(\theta_n)\hat{i} + \cos(\theta_n)\hat{j}\right], \tag{6}$$

where $\hat{i}$ and $\hat{j}$ represent the unit vectors with respect to the X and Y axis, respectively. The above expressions allow us to obtain the position of the particle as a function of time for $t \geqslant t_n$:

$$X_p(t) = X(\delta_n, t_n) - \sin(\theta_n)\left[|\vec{V}_n| - \frac{1}{2}\mu(t - t_n)\right](t - t_n), \tag{7}$$

$$Y_p(t) = Y(\delta_n, t_n) + \cos(\theta_n)\left[|\vec{V}_n| - \frac{1}{2}\mu(t - t_n)\right](t - t_n). \tag{8}$$

The index p denotes that such coordinates correspond to the particle. In order to know the position of the particle at the $(n+1)$th collision we need to solve numerically the following equation

$$\sqrt{\left[l_x - X_p(t)\right]^2 + \left[l_y - Y_p(t)\right]^2} \cong R, \tag{9}$$

where l_x and l_y are the X and Y components of $l(s_n)$ and this distance is measured from the origin of the coordinates system to the center of the $s_n = 0, \ldots, 11$ scatters at $(n+1)$th collision. Since the position of the particle at the collision $(n+1)$th is known, one can easily obtain the instant of collision by evaluation $t_{n+1} = t_n + t_c$ where t_c is the time during the flight.

The impact parameter, b_{n+1}, which is perpendicular to the particle's trajectory, is obtained geometrically as can be seen in Fig. 2(b) and it is written as

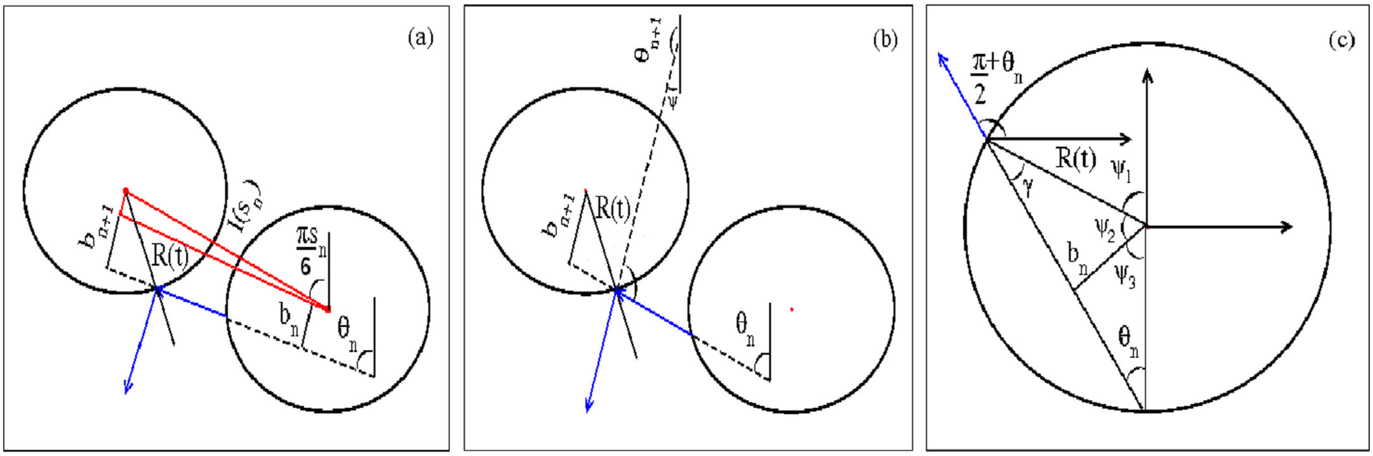

Fig. 2. (a) Position of the particle on the boundary for each collision; (b) b_{n+1} on b_n and θ_n; Dependence of (c) θ_{n+1} on b_{n+1} and θ_n.

$$b_{n+1} = b_n - l(s_n)\sin\left(\theta_n - \frac{\pi s_n}{6}\right). \tag{10}$$

Since the referential frame of the boundary is moving, then, at the instant of the collision, according to our construction, the following conditions must be matched

$$\vec{V}'_{n+1} \cdot \vec{T}_{n+1} = \vec{V}'_p \cdot \vec{T}_{n+1}, \tag{11}$$

$$\vec{V}'_{n+1} \cdot \vec{N}_{n+1} = -\vec{V}'_p \cdot \vec{N}_{n+1}, \tag{12}$$

where $\vec{T}_{n+1}$ and $\vec{N}_{n+1}$ tangent and normal unity vectors, respectively. The upper prime indicates that the velocity of the particle is measured with respect to the moving boundary referential frame.

Hence, one can easily find that

$$\vec{V}_{n+1} \cdot \vec{T}_{n+1} = \vec{V}_p \cdot \vec{T}_{n+1}, \tag{13}$$

$$\vec{V}_{n+1} \cdot \vec{N}_{n+1} = -\vec{V}_p \cdot \vec{N}_{n+1} + 2\vec{V}_b(t_{n+1}) \cdot \vec{N}_{n+1}, \tag{14}$$

where $\vec{V}_b(t_{n+1}) = -\epsilon\sin(t_{n+1})$ is the velocity of the boundary.

Finally, the velocity at $(n+1)$th collision is

$$|\vec{V}_{n+1}| = \sqrt{(\vec{V}_{n+1} \cdot \vec{T}_{n+1})^2 + (\vec{V}_{n+1} \cdot \vec{N}_{n+1})^2}. \tag{15}$$

With such a four-dimensional map we can describe the dynamics of a time-dependent dissipative Lorentz gas. However, before starting with the time-dependent model, let us consider the case of $\epsilon = 0$ and $V_0 = 1$. For such a case, the velocity is a constant and the phase space is fully chaotic as can be seem in Fig. 3. Here, colors represent collisions with different scatterers as labeled in the figure. Therefore, according to LRA-conjecture, after the introduction of a time-dependent perturbation on the boundary the unlimited energy growth must be observed for the conservative dynamics.

3. Numerical results

Our numerical results for the time-dependent Lorentz gas consider basically the behavior of the average velocity of the particle. We use two different procedures to obtain the average velocity, namely, we first evaluate the average velocity over the orbit for a single initial condition which is defined as

$$V_i = \frac{1}{n+1}\sum_{j=0}^{n} V_{i,j}, \tag{16}$$

where the index i corresponds to a sample of an ensemble of initial conditions. Hence, the average velocity is written as

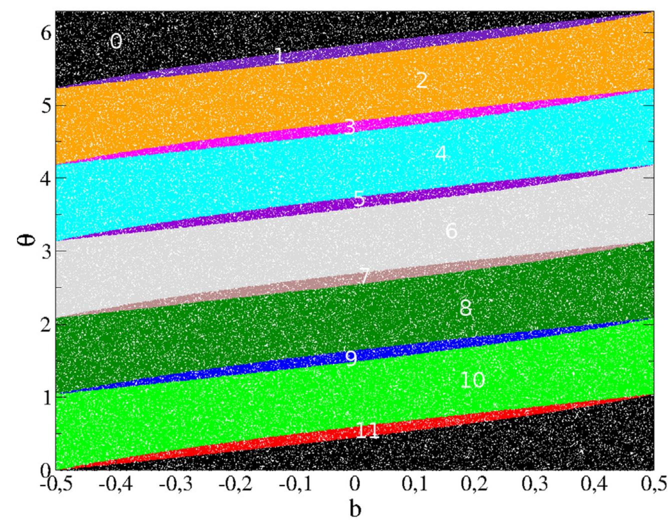

Fig. 3. Fully chaotic phase space for the time-independent case ($\epsilon = 0$). Colors represent the scatterer at collision $n+1$.

$$\overline{V} = \frac{1}{M}\sum_{i=1}^{M} V_i, \tag{17}$$

where M denotes the number of different initial conditions. We have considered $M = 200$ in our simulations.

Fig. 4 shows the parameter space for the dissipative Lorentz gas. The procedure used to construct the figure was to divide both $\mu \in [10^{-4}, 0.05]$ and $\epsilon \in [10^{-4}, 0.07]$ into windows of 600 parts each, thus leading to a total of 3.6×10^5 different combination of the control parameters. Starting with a fixed initial velocity $V_0 = 0.1$ and randomly chose $t_0 \in [0, 2\pi]$, $\delta_0 \in [0, 2\pi]$ and $b_0 \in [-1 - \epsilon\cos(t_0), 1 + \epsilon\cos(t_0)]$, we iterated Eq. (17) up to 10^5 for the ensemble of initial conditions and for each combination of μ and ϵ we saved the last values for the average velocity. The average velocity are coded with a continuous color scale ranging from green-blue for these parameters where the average velocity increased ($\overline{V} > V_0$) and red-yellow for these parameter whose average velocity decreased ($\overline{V} < V_0$) and eventually will come to a complete stop between the scatterers. As one can see, even for the dissipative dynamics, for some cases the average velocity increases up to 30 after 10^5 collisions, which is 300 times bigger then the initial velocity.

In order to confirm if the unlimited energy growth is observed in a dissipative system, we study the behavior of the average velocity as a function of the number of collisions with the scatterers

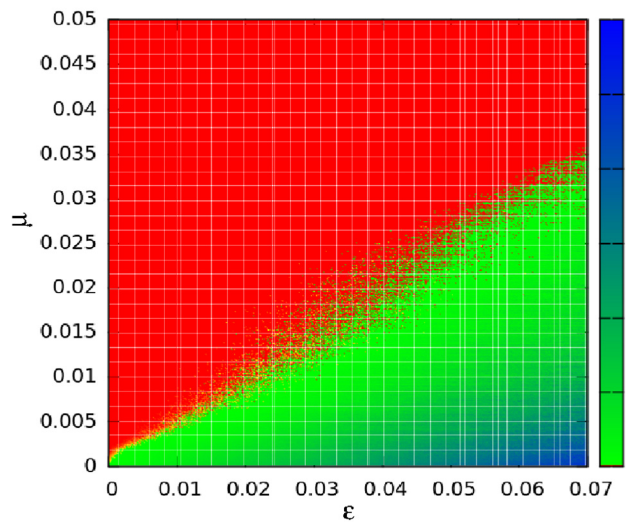

Fig. 4. Parameter space for the time-dependent Lorentz gas.

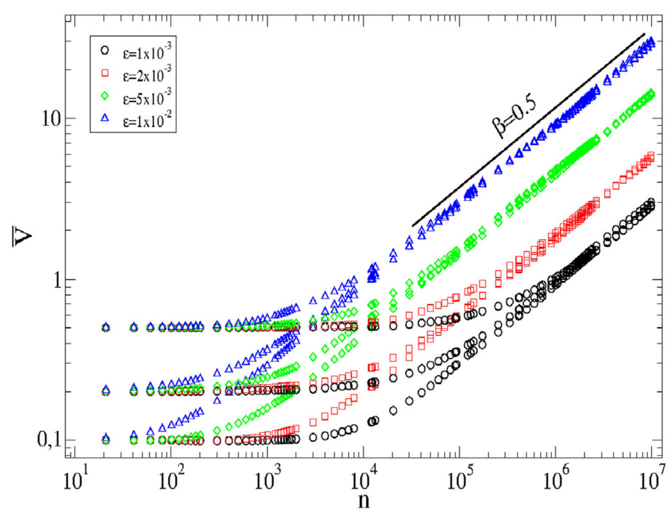

Fig. 5. Behavior of $\overline{V} \times n$ for different values of ϵ, as labeled in the figure and three different initial velocities, namely $V_0 = 0.1, 0.2$ and 0.5.

for different values of the initial velocity and different amplitudes ϵ as it is shown in Fig. 5. For each initial condition we have fixed the initial velocity, $V_0 \in [0.1, 10]$ and randomly chose $t_0 \in [0, 2\pi]$, $\delta_0 \in [0, 2\pi]$ and $b_0 \in [-1 - \epsilon\cos(t_0), 1 + \epsilon\cos(t_0)]$. The dissipation parameter μ were fixed as $\mu = 10^{-3}$. Note that, the average velocity for all values of ϵ and considering small values of n remains constant and then it starts to grow with the same exponent. The changeover from constant velocity to growth is marked by a crossover number n_x which is basically the intersection between the line of the initial plateau and the acceleration line. Additionally, the behavior shown in Fig. 5 is typical in systems that can be described by using scaling arguments. Therefore, we can propose the following scaling hypotheses:

1. When $n \ll n_x$ the average velocity is
$$\overline{V}_{ip} \propto V_0^{\alpha}, \tag{18}$$
where α is the exponent of the initial plateau and if it is well defined α must be equal to one;
2. For long time, $n \gg n_x$, the growth of the average velocity is described as
$$\overline{V} \propto n^{\beta}, \tag{19}$$
where β is the acceleration exponent;
3. The crossover number that marks the regime of growth to the constant velocity is written as
$$n_x \propto V_0^{z}\epsilon^{\gamma}, \tag{20}$$
where z and γ are the crossover exponents.

After considering the above scaling hypotheses, we propose a scaling function to describe the behavior of the average velocity of the type
$$\overline{V}[V_0, n, \epsilon] = \lambda\overline{V}\big[\lambda^{a}V_0, \lambda^{b}n, \lambda^{c}\epsilon\big], \tag{21}$$
where a, b and c are scaling exponents and λ is a scaling factor. Since λ is a scaling factor, we can chose it such that $\lambda^{a}V_0 = 1$, yielding to $\lambda = V_0^{-1/a}$, thus Eq. (21) can be rewritten as
$$\overline{V}[V_0, n, \epsilon] = V_0^{-1/a}\overline{V}\big[1, V_0^{-b/a}, V_0^{-c/a}\epsilon\big]. \tag{22}$$
Comparing Eq. (18) and Eq. (22), we obtain $\alpha = -1/a$. On the other hand, by choosing now $\lambda^{b}n = 1$, we have that $\lambda = n^{-1/b}$ and Eq. (21) is rewritten as
$$\overline{V}[V_0, n, \epsilon] = n^{-1/b}\overline{V}\big[n^{-a/b}V_0, 1, n^{-c/b}\epsilon\big]. \tag{23}$$
Comparing now Eq. (19) and Eq. (23), we obtain $\beta = -1/b$. Choosing $\lambda^{c}\epsilon = 1$, we have that $\lambda = \epsilon^{-1/c}$. Using now the expressions obtained for the scaling factor λ, and the two conditions for the crossover, namely $V_0^{-1/a} = \lambda = n^{-1/b}$ and $n^{-1/b} = \lambda = \epsilon^{-1/c}$ one can easily conclude that $z = \frac{\alpha}{\beta}$ and $\gamma = -1/c\beta$. Since we have all the relationship between the exponents, in order to confirm our scaling hypotheses we need to find their values numerically. The acceleration exponent β, is obtained from a power law fitting for the average velocity when $n \gg n_x$. Thus, an average of these values gives us $\beta = 0.502(3)$. Fig. 6 shows the behavior of (a) $\overline{V}_{ip}$ vs. V_0 and (b), n_x vs. V_0. After power law fittings we obtain $\alpha = 0.9997(4) \cong 1$ and $z = 1.991(2) \cong 2$. The crossover exponent z can also be obtained by using the previous values of the acceleration exponent β and the exponent of the initial plateau α. Thus we find $z = \frac{\alpha}{\beta} = 1.99(1)$ which is in excellent agreement with the our numerical data. Finally, Fig. 6(c) shown the behavior of n_x vs. ϵ, after a power law fitting we obtained $\gamma = -2.00(2)$.

A final check of the initial hypotheses and our scaling exponents will be done in two steps. As one can see in Fig. 5 the behavior of the average velocities highly depends on the initial velocity V_0 and the amplitude of the time-dependent perturbation ϵ, here we have considered three different values for V_0 and four different amplitudes. First let us assume that the ϵ is fixed, therefore, one must consider the following transformation $\overline{V} \mapsto \overline{V}/V_0^{\alpha}$ and $n \mapsto n/V_0^{z}$ and as it is shown in Fig. 7(a) four collapses happened, one for each value of ϵ. Finally, the final collapse is done by considering the dependence of the average velocity also on ϵ. As one can see in Fig. 7(b) all the curves collapse onto a single and universal plot. Such a result allow us to confirm that the system is scaling invariant with scaling exponents very well defined. Additionally, we have shown for the first time for a two-dimensional time-dependent billiard that the unlimited energy growth is possible even if the system is dissipative.

4. Conclusion

We have studied the problem of a classical particle experiencing collisions with time-dependent circular scatterers. We have obtained the four-dimensional map that describes the dynamics of the dissipative system. We have studied parameter space by using the behavior of the average velocity for an ensemble of initial

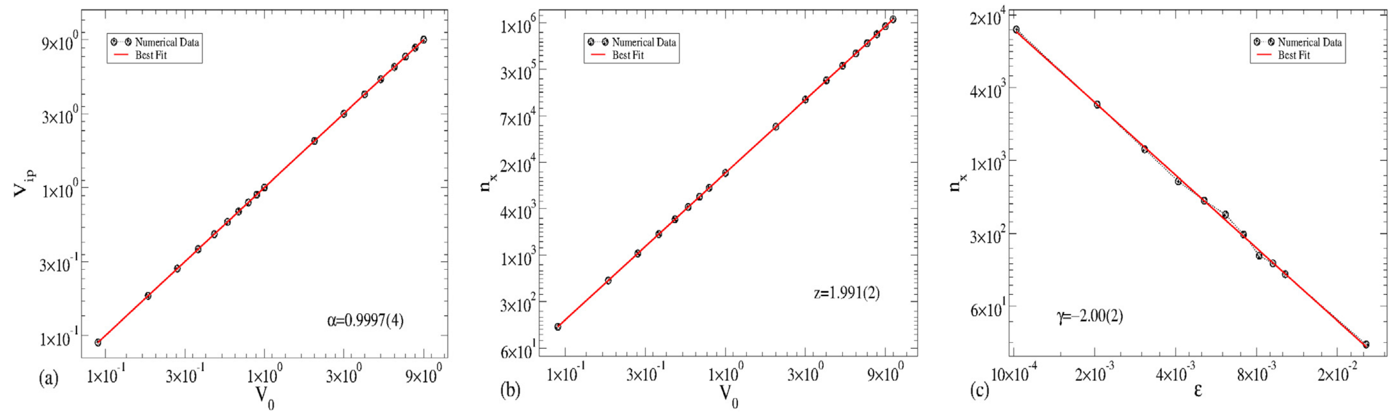

Fig. 6. (a) Behavior of $\overline{V}_{ip}$ vs. V_0. (b) Behavior of the crossover number n_x against V_0 and (c) behavior of n_x vs. ϵ A power law fitting in (a) furnishes $\alpha = 0.9997(4)$ while in (b) $z = -1.991(2)$ and (c) $\gamma = -2.00(2)$.

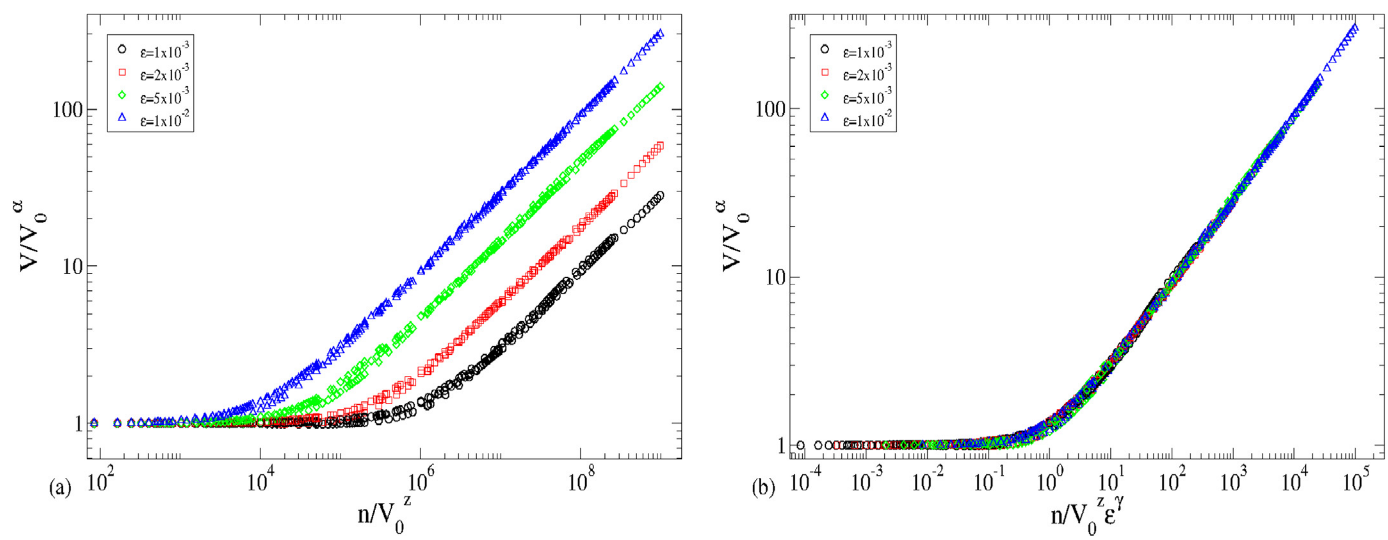

Fig. 7. Different curves of the $\overline{V}$ for different values of ϵ and different initial velocities. (a) Their initial collapse onto four different which depends on ϵ. (b) Their final collapse onto a single and universal plot.

conditions and we have shown that for some combination of initial condition and control parameters the unlimited energy growth in completely suppressed and the particles come to a complete stop between the scatterers. On the other hand, for some other combinations of control parameters the average velocity grows unbounded. For such a case, the behavior of the average energy has been considered in the framework of scaling. Once the acceleration exponent β, the exponent of the initial plateau α and the two crossover exponents z and γ have been obtained, the scaling hypotheses are confirmed by the perfect collapse of all curves onto a single universal plot. Additionally, we have shown for the first time in a two-dimensional time-dependent billiard that the unlimited energy growth is observed in a dissipative system.

Acknowledgements

This work was supported by the Deutsche Forschungsgemeinschaft through the Cluster of Excellence Engineering of Advanced Materials.

References

[1] E. Fermi, On the origin of the cosmic radiation, Phys. Rev. 75 (1949) 1169.
[2] S.E. Sklarz, D.J. Tannor, N. Khaneja, Decoherence control by tracking a Hamiltonian reference molecule, Phys. Rev. A 69 (2004) 053408.
[3] R. Gommers, S. Bergamini, F. Renzoni, Dissipation-induced symmetry breaking in a driven optical lattice, Phys. Rev. Lett. 95 (2005) 073003.
[4] M. Steiner, M. Freitag, V. Perebeinos, J.C. Tsang, J.P. Small, M. Kinoshita, D. Yuan, J. Liu, P. Avouris, Phonon populations and electrical power dissipation in carbon nanotube transistors, Nat. Nanotechnol. 4 (2009) 320.
[5] K. Nakamura, T. Harayama, Quantum Chaos and Quantum Dots, Oxford University Press, Oxford, 2004.
[6] S.O. Kamphorst, S. Pinto de Carvalho, Bounded gain of energy in the breathing circle billiard, Nonlinearity 12 (1999) 1363.
[7] J. Koiller, R. Markarian, S.O. Kamphorst, S. Pinto de Carvalho, Static and time-dependent perturbations of the classical elliptical billiard, J. Stat. Phys. 83 (1996) 127.
[8] L.A. Bunimovich, On the ergodic properties of nowhere dispersing billiards, Commun. Math. Phys. 65 (1979) 295.
[9] Y.G. Sinai, Dynamical systems with elastic reflections, Russian Math. Surveys 25 (1970) 137.
[10] M. Robnik, Classical dynamics of a family of billiards with analytic boundaries, J. Phys. A: Math. Gen. 16 (1983) 3971.
[11] N. Saitô, H. Hirooka, J. Ford, F. Vivaldi, G.H. Walker, Numerical study of billiard motion in an annulus bounded by non-concentric circles, Physica D 5 (1982) 273.
[12] M.V. Berry, Regularity and chaos in classical mechanics, illustrated by three deformations of a circular 'billiard', Eur. J. Phys. 2 (1981) 91.
[13] M.V. Berry, M. Robnik, Semiclassical level spacings when regular and chaotic orbits coexist, J. Phys. A 17 (1984) 2413.
[14] M. Robnik, Quantising a generic family of billiards with analytic boundaries, J. Phys. A 17 (1984) 1049.
[15] M. Robnik, M.V. Berry, Classical billiards in magnetic fields, J. Phys. A: Math. Gen. 18 (1985) 1361.

[16] J.K.L. da Silva, D.G. Ladeira, E.D. Leonel, P.V.E. McClintock, S.O. Kamphorst, Scaling properties of the Fermi–Ulam accelerator model, Braz. J. Phys. 36 (2006) 700.

[17] R. Markarian, S.O. Kamphorst, S.P. de Carvalho, Chaotic properties of the elliptical stadium, Commun. Math. Phys. 174 (1996) 661.

[18] V. Lopac, I. Mrkonjić, D. Radić, Classical and quantum chaos in the generalized parabolic lemon-shaped billiard, Phys. Rev. E 59 (1999) 303.

[19] V. Lopac, I. Mrkonjić, D. Radić, Chaotic behavior in lemon-shaped billiards with elliptical and hyperbolic boundary arcs, Phys. Rev. E 66 (2001) 036202.

[20] E.D. Leonel, P.V.E. McClintock, A hybrid Fermi–Ulam-bouncer model, J. Phys. A 38 (2005) 823.

[21] A.M. Ozorio de Almeida, Hamiltonian Systems: Chaos and Quantization, Cambridge Univ. Press, Cambridge, 1988.

[22] A. Loskutov, A.R. Ryabov, L.G. Akinshin, Properties of some chaotic billiards with time-dependent boundaries, J. Phys. A: Math. Gen. 33 (2000) 7973.

[23] V. Gelfreich, D. Turaev, Unbounded energy growth in Hamiltonian systems with a slowly varying parameter, Comm. Math. Phys. 283 (2008) 769.

[24] V. Gelfreich, D. Turaev, Fermi acceleration in non-autonomous billiards, J. Phys. A 41 (2008) 212003.

[25] A.L.P. Livorati, A. Loskutov, E.D. Leonel, A peculiar Maxwell's Demon observed in a time-dependent stadium-like billiard, Physica A 391 (2012) 4756.

[26] E.D. Leonel, D.F.M. Oliveira, A. Loskutov, Fermi acceleration and scaling properties of a time dependent oval billiard, Chaos 19 (2009) 033142.

[27] E.D. Leonel, L.A. Bunimovich, Suppressing Fermi acceleration in a driven elliptical billiard, Phys. Rev. Lett. 104 (2010) 224101.

[28] F. Lenz, F.K. Diakonos, P. Schmelcher, Tunable Fermi acceleration in the driven elliptical billiard, Phys. Rev. Lett. (2008) 100: 203.

[29] F. Lenz, C. Petri, F.R.N. Koch, F.K. Diakonos, P. Schmelcher, Evolutionary phase space in driven elliptical billiards, New J. Phys. 11 (2009) 083035.

[30] F. Lenz, C. Petri, F.K. Diakonos, P. Schmelcher, Phase-space composition of driven elliptical billiards and its impact on Fermi acceleration, Phys. Rev. E 82 (2010) 016206.

[31] D.F.M. Oliveira, M. Robnik, In-flight dissipation as a mechanism to suppress Fermi acceleration, Phys. Rev. E 83 (2011) 026202.

[32] D.F.M. Oliveira, M. Robnik, Scaling invariance in a time dependent elliptical billiard, Int. J. Bifur. Chaos 22 (2012) 1250207.

[33] C. Grebogi, E. Ott, J.A. Yorke, Chaotic attractors in crisis, Phys. Rev. Lett. 48 (1982) 1507.

[34] C. Grebogi, E. Ott, J.A. Yorke, Crises, sudden changes in chaotic attractors, and transient chaos, Physica D 7 (1983) 181.

[35] E.D. Leonel, P.V.E. McClintock, A crisis in the dissipative Fermi accelerator model, J. Phys. A 38 (2005) L425.

[36] M. Feigenbaum, Quantitative universality for a class of nonlinear transformations, J. Stat. Phys. 19 (1978) 25.

[37] M. Feigenbaum, The universal metric properties of nonlinear transformations, J. Stat. Phys. 21 (1979) 669.

[38] J.A.C. Gallas, Structure of the parameter space of the Hénon map, Phys. Rev. Lett. 70 (1993) 2714.

[39] J.A.C. Gallas, Structure of the parameter space of a ring cavity, Appl. Phys. B 60 (1994) S203.

[40] J.A.C. Gallas, Dissecting shrimps: results for some one-dimensional physical systems, Physica A 202 (1994) 196.

[41] R. Gommers, S. Bergamini, F. Renzoni, Dissipation induced symmetry breaking in an driven optical lattice, Phys. Rev. Lett. 95 (2005) 073003.

[42] J.K. Bhattacharjee, D. Thirumalai, Drag reduction in turbulent flows by polymers, Phys. Rev. Lett. 67 (1991) 196.

[43] Y. Zhao, C. Ma, G. Chen, Q. Jiang, Energy dissipation mechanisms in carbon nanotube oscillators, Phys. Rev. Lett. 91 (2003) 175504.